Hybrid Beamforming Design for ITS-assisted Wireless Networks

Wannian Du, Zheng Chu, *Member, IEEE,* Gaojie Chen, *Senior Member, IEEE,*
Pei Xiao, *Senior Member, IEEE,* Zihuai Lin, *Senior Member, IEEE,*
Cheng Huang, and Wanming Hao, *Member, IEEE*

***Abstract*—This letter proposes a hybrid beamforming design for an intelligent transmissive surface (ITS)-assisted transmitter wireless network. We aim to suppress the sidelobes and optimize the mainlobes of the transmit beams by minimizing the proposed cost function based on the least squares (LS) for the digital beamforming vector of the base station (BS) and the phase shifts of the ITS. To solve the minimization problem, we adopt an efficient algorithm based on the alternating optimization (AO) method to design the digital beamforming vector and the phase shifts of the ITS in an alternating manner. In particular, the alternating direction method of multipliers (ADMM) algorithm is utilized to obtain the optimal phase shifts of the ITS. Finally, we verify the improvement achieved by the proposed algorithm in terms of the beam response compared to the benchmark schemes by the simulation results.**

***Index Terms*—ITS, hybrid beamforming design, AO, ADMM.**

I. Introduction

MASSIVE multiple-input multiple-output (MIMO) systems are one of the essential technologies for the beyond-fifth-generation (B5G) and six-generation (6G) wireless communications. However, a large number of radio frequency (RF) chains connected to active antennas in the conventional fully-digital transmitter will incur huge power consumption and high complexity, which has motivated the work on hybrid analog-digital beamforming structures [1–4] to decrease the number of RF chains by moving some signal processing operations into the analogue domain. However, the undesired high sidelobes may be caused in these hybrid beamforming structures. Hence, to mitigate the adverse effect of the sidelobes in the transmit beam, different techniques were proposed in the hybrid beamforming architecture [5–7]. Nevertheless, the cost of the analog network in conventional hybrid beamforming structures is still high for the massive number of RF components, such as dividers, combiners, phase shifters and the connections between them, which calls for more effective and innovative solutions [8].

Fortunately, the technologies of the meta-surfaces and state-of-the-art manufacturing have been developed rapidly, and the ITS, which is equipped with massive low-cost passive elements, could be an effective replacement for conventional hybrid beamforming structures. The main advantage of the ITS-aided transceiver architecture is that the high-cost power amplifiers and RF chains can be replaced by passive elements in the ITS [9]. This inspired studies on adopting an ITS in a transceiver architecture [8, 10, 11]. Although the ITS-assisted transmitter architecture can effectively reduce the costs of the analog network compared to conventional hybrid beamforming structures, the undesired high sidelobes in the transmit beam still exist, which calls for effective solutions. However, there does not exist any work in the literature addressing sidelobe suppression in wireless systems with an ITS-aided transmitter.

Against this background, we propose a novel hybrid beamforming design for an ITS-assisted network and consider the solution to suppress the effect of the sidelobes in the transmit beam. To the best of the authors' knowledge, this work is the first of its kind to suppress the effect of the sidelobes in the hybrid beamforming design with the aid of an ITS. The main contributions of this paper include: 1) In this letter, we consider a minimization problem of a cost function based on LS for the transmit beam, which can suppress the sidelobes and maximize the mainlobes. Also, the mainlobes are optimized to point to the users at arbitrary directions; 2) To solve the non-convex minimization problem, which is related to the optimal digital beamforming vector at the BS and the phase shifts of the ITS, we propose an efficient algorithm based on the AO and ADMM method; 3) Simulation results verify the convergence of the proposed algorithm and demonstrate the superiority of the proposed scheme over other benchmark schemes.

II. System model and problem formulation

We consider an ITS-assisted network where the transmitter consists of a BS with N active antennas and an ITS with M passive elements, and there are K users receiving transmit

This work was supported in part by the U.K. Engineering and Physical Sciences Research Council (EPSRC) under Grant EP/P03456X/1 and EP/X013162/1. The work of Wanming Hao was supported in part by the China National Natural Science Foundation under Grant 62101499 and in part by the SongShan Laboratory Foundation under Grant YYJC022022003. (*Corresponding author: Zheng Chu, Gaojie Chen.*)

Wannian Du is with School of Automation, Nanjing University of Science and Technology, Nanjing 210094, China and Institute for Communication Systems (ICS), Home for 5GIC & 6GIC, University of Surrey, Guildford, Surrey, GU2 7XH, United Kingdom. (Email: (wanniandd@gmail.com).

Zheng Chu, Gaojie Chen and Pei Xiao are with the Institute for Communication Systems (ICS), Home for 5GIC & 6GIC, University of Surrey, Guildford, Surrey, GU2 7XH, United Kingdom. (Email: andrew.chuzheng7@gmail.com, gaojie.chen@surrey.ac.uk and p.xiao@surrey.ac.uk).

Zihuai Lin is with School of Electrical & Information Engineering, The University of Sydney, Sydney, NSW 2006, Australia. (Email: zihuai.lin@sydney.edu.au).

Cheng Huang is with School of Automation, Nanjing University of Science and Technology, Nanjing, 210094, China. (Email: hearthc@163.com).

Wanming Hao is with the School of Electrical and Information Engineering, Zhengzhou University, Zhengzhou 450001, China, and also with the SongShan Laboratory, Zhengzhou 450018, China (e-mail: iewmhao@zzu.edu.cn).

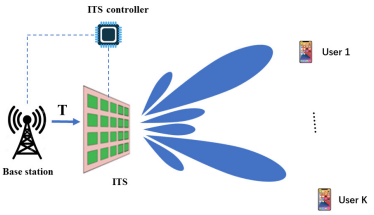

Fig. 1: System model with ITS-aided transmitter.

beams from an ITS-assisted transmitter as shown in Fig. 1. In the transmitter, each active antenna at BS is connected to a dedicated RF chain and transmits the signal to the ITS. Consequently, the design of the beamforming vector in the conventional fully-digital transmitter is transformed into the joint design of the digital beamforming at the BS and the phase shifts of ITS elements. Thus, there is no direct link between the ITS and the users. The diagonal matrix $\boldsymbol{\Theta}_T$ related to the phase shifts of the ITS with continuous values is expressed as:

$$\boldsymbol{\Theta}_T = \text{diag}\left(e^{j\alpha_1^{(t)}}, ..., e^{j\alpha_M^{(t)}}\right),\ \alpha_m^{(t)} \in [-\pi, \pi), \forall m \in [1, M]. \tag{1}$$

We adopt the uniform separate illumination (USI) strategy as studied in [8] to describe the illumination channel between the BS and the ITS. In the USI strategy, each part of the intelligent surface only receives the signal from one active antenna and the powers of the received signals are identical. The uniform power distribution in the USI strategy results in a higher antenna gain of the ITS compared to other illumination strategies. The illumination channel between the BS and the ITS, i.e., $\mathbf{T}$, is described as follows:

$$\mathbf{T} = \left[\boldsymbol{\chi} e^{-j\frac{2\pi r_{m,n}}{\lambda}}\right]_{m,n}, \tag{2}$$

where

$$\boldsymbol{\chi} = \begin{cases} \frac{\lambda M}{4\pi\left(\sum_n \sum_{m\in\widetilde{M}} r_{m,n}\right)} \sqrt{\frac{4\pi\nu}{1-\cos(\theta_0^{\max})}} & m \in \widetilde{M} \\ 0 & \text{otherwise} \end{cases}, \tag{3}$$

where $n \in [1, N]$, $m \in [1, M]$, λ denotes the wavelength, ν is the efficiency factor of the ITS, $\widetilde{M}$ represents a set of the selected passive elements, which are connected to the active antenna n, and $\theta_0^{\max}$ is the elevation angle in the separate illumination (SI) strategy.

In addition, the ITS is modeled as an M-element uniform planar array (UPA), with M_x row elements and M_y column elements. We consider that all elements are equally spaced at the ITS and the distance between two elements is $d = \frac{\lambda}{2}$. Thus, the steering vector $\boldsymbol{s}(\delta, \phi)$ at the ITS can be described as in (4), where $\delta \in \boldsymbol{\delta}_{all}$ and $\phi \in \boldsymbol{\phi}_{all}$. $\boldsymbol{\delta}_{all} = [-\frac{\pi}{2}, \frac{\pi}{2})$ and $\boldsymbol{\phi}_{all} = [-\frac{\pi}{2}, \frac{\pi}{2})$ are the ranges of the elevation angle and azimuth angle, respectively.

$$\boldsymbol{s}(\delta, \phi) = \left[1, e^{j2\pi\frac{d}{\lambda}\sin\delta}, ..., e^{j2\pi\left(\frac{(M_x-1)d}{\lambda}\sin\phi\cos\delta + \frac{(M_y-1)d}{\lambda}\sin\delta\right)}\right]^T. \tag{4}$$

Next, the beam response transmitted from the ITS-assisted transmitter can be shown as:

$$\mathcal{P}(\delta, \phi) = \boldsymbol{s}(\delta, \phi)^H \boldsymbol{\Theta}_T \mathbf{T} \boldsymbol{w}, \tag{5}$$

where $\boldsymbol{w} \in \mathbb{C}^{N\times 1}$ is the digital beamforming vector at the BS.

To suppress the effect of the sidelobes and improve the performance of K mainlobes intended for K users in the beam response with the help of the ITS-assisted transmitter, we consider the following cost function based on LS in [12] for the transmit beam:

$$J_{LS} = \int_{\delta\in\boldsymbol{\delta}_{all}} \int_{\phi\in\boldsymbol{\phi}_{all}} F(\delta, \phi)|H(\delta, \phi) - D(\delta, \phi)|^2 \,\mathrm{d}\delta\mathrm{d}\phi, \tag{6}$$

where $F(\delta, \phi)$ is a positive real weighting function to represent the importance of certain region in the cost function. In addition, $H(\delta, \phi)$ and $D(\delta, \phi)$ are the designed and desired beam response of the transmit beam, respectively. Specially, $D(\delta, \phi) = 0$ in the sidelobe region. We consider that the angles in $\boldsymbol{\delta}_{all}$ and $\boldsymbol{\phi}_{all}$ are discrete values. Let $\boldsymbol{\delta}_m$ and $\boldsymbol{\phi}_m$ denote the sets of angles in mainlobes. Also, $\boldsymbol{\delta}_s$ and $\boldsymbol{\phi}_s$ denote the sets in sidelobes. Substituting the designed beam response $\mathcal{P}(\delta, \phi)$ into (6), the formulation of J_{LS} can be rewritten as:

$$\begin{aligned} J_{LS} =& (1-\beta) \sum_{\delta\in\boldsymbol{\delta}_m, \phi\in\boldsymbol{\phi}_m} |\mathcal{P}(\delta, \phi) - D(\delta, \phi)|^2 \\ &+ \frac{\beta}{N_s} \sum_{\delta\in\boldsymbol{\delta}_s, \phi\in\boldsymbol{\phi}_s} |\mathcal{P}(\delta, \phi)|^2, \end{aligned} \tag{7}$$

where $\beta \in (0, 1)$ is a trade-off parameter to represent the importance of the mainlobe and sidelobe in J_{LS}. Also, N_s is the number of the sidelobes.

To minimize the cost function J_{LS}, we can consider the following optimization problem:

$$\min_{\boldsymbol{\Theta}_T, \boldsymbol{w}} \quad J_{LS} \tag{8a}$$

$$\text{s.t. } C1 : (1), \tag{8b}$$

$$C2 : \boldsymbol{w}^H \boldsymbol{w} \le P_{\max}. \tag{8c}$$

In the above optimization problem, $C1$ denotes the constraints of the phase shifts of ITS. The $P_{\max}$ in $C2$ denotes the transmit power budget at the BS. We aim to minimize the cost function by joint design of the digital beamforming vector $\boldsymbol{w}$ and the phase shifts $\boldsymbol{\Theta}_T$. However, problem (8) is intractable due to its non-convexity caused by the coupling of the two variables. Next, we propose an effective algorithm to solve the optimization problem.

III. Problem Solution

To decouple $\boldsymbol{w}$ and $\boldsymbol{\Theta}_T$ in problem (8), we adopt the AO method to optimize the variables in an alternating manner.

A. Optimization of $\boldsymbol{w}$

We first consider the optimization of $\boldsymbol{w}$ with a given $\boldsymbol{\Theta}_T$. Let $\boldsymbol{b}(\delta, \phi) = \boldsymbol{s}(\delta, \phi)^H \boldsymbol{\Theta}_T \mathbf{T}$ and introduce the Lagrangian multiplier μ related to the constraint $C2$, the Lagrangian function $\mathcal{L}(\boldsymbol{w})$ can be described as (9) at the top of the next page, which is a convex function over $\boldsymbol{w}$. Thus, the optimal value of $\boldsymbol{w}$ can be obtained by setting $\partial\mathcal{L}(\boldsymbol{w})/\partial\boldsymbol{w}$ to zero as shown in (10) at the top of the next page. Especially, if the constraint $C2$ is not met with equality at $\tilde{\boldsymbol{w}}$, the optimal value of μ is $\tilde{\mu} = 0$. Thus, the optimal solution is $\tilde{\boldsymbol{w}}(0)$. Otherwise, the optimal value of μ is given by (11), which can be obtained by the bisection search method, and then the optimal value of $\boldsymbol{w}$ can be obtained in (10) with the optimal value of μ.

$$\tilde{\mu} = \left\{\mu \ge 0 : \boldsymbol{w}(\mu)^H \boldsymbol{w}(\mu) = P_{\max}\right\}. \tag{11}$$

$$\mathcal{L}(\boldsymbol{w}) =(1-\beta)\sum_{\delta\in\boldsymbol{\delta}_m,\phi\in\boldsymbol{\phi}_m}(\boldsymbol{b}(\delta,\phi)\boldsymbol{w})(\boldsymbol{b}(\delta,\phi)\boldsymbol{w})^H+\frac{\beta}{N_s}\sum_{\delta\in\boldsymbol{\delta}_s,\phi\in\boldsymbol{\phi}_s}(\boldsymbol{b}(\delta,\phi)\boldsymbol{w})(\boldsymbol{b}(\delta,\phi)\boldsymbol{w})^H$$
$$-2(1-\beta)\mathcal{R}\left\{\sum_{\delta\in\boldsymbol{\delta}_m,\phi\in\boldsymbol{\phi}_m}D(\delta,\phi)\boldsymbol{b}(\delta,\phi)\boldsymbol{w}\right\}+(1-\beta)\sum_{\delta\in\boldsymbol{\delta}_m,\phi\in\boldsymbol{\phi}_m}D(\delta,\phi)+\mu(\boldsymbol{w}^H\boldsymbol{w}-P_{\max}). \tag{9}$$

$$\tilde{\boldsymbol{w}}(\mu)=(1-\beta)\left(\sum_{\delta\in\boldsymbol{\delta}_m,\phi\in\boldsymbol{\phi}_m}(1-\beta)(\boldsymbol{b}^H\boldsymbol{b})+\frac{\beta}{N_s}\sum_{\delta\in\boldsymbol{\delta}_s,\phi\in\boldsymbol{\phi}_s}(\boldsymbol{b}^H\boldsymbol{b})+\mu\mathbf{I}\right)^{-1}\sum_{\delta\in\boldsymbol{\delta}_m,\phi\in\boldsymbol{\phi}_m}D(\delta,\phi)\boldsymbol{b}^H. \tag{10}$$

B. Optimization of $\boldsymbol{\Theta}_T$

After obtaining the optimal value of $\boldsymbol{w}$ the formulation of $\mathcal{P}(\delta,\phi)$ can be transformed as follows:

$$\begin{aligned}\mathcal{P}(\delta,\phi)&=\boldsymbol{s}(\delta,\phi)^H\boldsymbol{\Theta}_T\mathbf{T}\boldsymbol{w}\\&=\boldsymbol{\theta}_T\mathrm{diag}(\boldsymbol{s}(\delta,\phi)^H)\mathbf{T}\boldsymbol{w}\\&=\boldsymbol{\theta}_T\boldsymbol{a}(\delta,\phi,\boldsymbol{w}),\end{aligned} \tag{12}$$

where $\boldsymbol{\theta}_T=\left[\theta_1^{(t)},\theta_2^{(t)},...,\theta_M^{(t)}\right]=\left[e^{j\alpha_1^{(t)}},e^{j\alpha_2^{(t)}},...,e^{j\alpha_M^{(t)}}\right]$ is the diagonal vector of $\boldsymbol{\Theta}_T$ with $|\boldsymbol{\theta}_T(m)|=1,\ \forall m\in[1,M]$. Thus, the cost function is equivalent to:

$$J_{LS}=\boldsymbol{\theta}_T\boldsymbol{\Phi}\boldsymbol{\theta}_T^H-2\mathcal{R}\left\{\boldsymbol{\theta}_T\boldsymbol{\Psi}\right\}+q, \tag{13}$$

where

$$\begin{aligned}\boldsymbol{\Phi}&=(1-\beta)\sum_{\delta\in\boldsymbol{\delta}_m,\phi\in\boldsymbol{\phi}_m}\boldsymbol{a}(\delta,\phi,\boldsymbol{w})\boldsymbol{a}(\delta,\phi,\boldsymbol{w})^H\\&\quad+\frac{\beta}{N_s}\sum_{\delta\in\boldsymbol{\delta}_s,\phi\in\boldsymbol{\phi}_s}\boldsymbol{a}(\delta,\phi,\boldsymbol{w})\boldsymbol{a}(\delta,\phi,\boldsymbol{w})^H\\\boldsymbol{\Psi}&=(1-\beta)\sum_{\delta\in\boldsymbol{\delta}_m,\phi\in\boldsymbol{\phi}_m}D(\delta,\phi)\boldsymbol{a}(\delta,\phi,\boldsymbol{w})\\q&=(1-\beta)\sum_{\delta\in\boldsymbol{\delta}_m,\phi\in\boldsymbol{\phi}_m}D(\delta,\phi),\end{aligned} \tag{14}$$

and the last term q is independent of $\boldsymbol{\theta}_T$. Thus, to obtain the optimal value of $\boldsymbol{\theta}_T$, we only need to tackle the following optimization problem:

$$\min_{\boldsymbol{\theta}_T}\quad\boldsymbol{\theta}_T\boldsymbol{\Phi}\boldsymbol{\theta}_T^H-2\mathcal{R}\left\{\boldsymbol{\theta}_T\boldsymbol{\Psi}\right\} \tag{15a}$$
$$\text{s.t. } C3:|\boldsymbol{\theta}_T(m)|=1,\ \forall m\in[1,M]. \tag{15b}$$

The problem (15a) remains intractable due to the unit modulus constraint $C3$, but can be solved by successive convex approximation (SCA), element-by-element iterative strategy and ADMM algorithms [13]. The ADMM has a lower complexity compared to the SCA method and a faster convergence compared to the element-by-element iterative strategy. Thus, we can adopt the ADMM algorithm studied in [14] to solve the problem (15a). We first introduce a slack variable $\boldsymbol{r}\in\mathbb{C}^{M\times1}$ to transform the problem (15a) into the ADMM framework as follows:

$$\min_{\boldsymbol{r},\boldsymbol{\theta}_T}\quad\boldsymbol{r}\boldsymbol{\Phi}\boldsymbol{r}^H-2\mathcal{R}\left\{\boldsymbol{r}\boldsymbol{\Psi}\right\} \tag{16a}$$
$$\text{s.t. } C3. \tag{16b}$$
$$\boldsymbol{r}=\boldsymbol{\theta}_T. \tag{16c}$$

The ADMM algorithm is based on the *augmented Lagrangian* as follows:

$$\begin{aligned}\mathcal{L}(\boldsymbol{r},\boldsymbol{\theta}_T,\boldsymbol{p})&=\boldsymbol{r}\boldsymbol{\Phi}\boldsymbol{r}^H-2\mathcal{R}\left\{\boldsymbol{r}\boldsymbol{\Psi}\right\}\\&\quad-\mathcal{R}\left\{\boldsymbol{p}^H(\boldsymbol{r}-\boldsymbol{\theta}_T)\right\}+\frac{\rho}{2}||\boldsymbol{r}-\boldsymbol{\theta}_T||^2,\end{aligned} \tag{17}$$

where $\rho\geq0$ is the penalty parameter and $\boldsymbol{p}\in\mathbb{C}^M$ is the Lagrange multiplier.

Then, we can consider the iteration optimization between the variables in (17) by the ADMM algorithm, which can be performed based on the following subproblems and the update for $\boldsymbol{p}$ as follows:

$$\boldsymbol{\theta}_T^{i+1}=\arg\min_{\boldsymbol{\theta}_T,\ \text{s.t.}C2}\mathcal{L}(\boldsymbol{r}^i,\boldsymbol{\theta}_T^i,\boldsymbol{p}^i), \tag{18a}$$
$$\boldsymbol{r}^{i+1}=\arg\min_{\boldsymbol{r}}\mathcal{L}(\boldsymbol{r}^i,\boldsymbol{\theta}_T^{i+1},\boldsymbol{p}^i), \tag{18b}$$
$$\boldsymbol{p}^{i+1}=\boldsymbol{p}^i-\rho(\boldsymbol{r}^{i+1}-\boldsymbol{\theta}_T^{i+1}), \tag{18c}$$

where i represents the number of iterations and $(\boldsymbol{r}^0,\boldsymbol{\theta}_T^0,\boldsymbol{p}^0)$ are the feasible initial variables as follows:

$$\begin{aligned}\boldsymbol{\theta}^0&=\mathrm{diag}\left(e^{j2\pi(1/M)},...,e^{j2\pi(M/M)}\right),\\\boldsymbol{r}^0&=\mathbf{0}\\\boldsymbol{p}^0&=\mathbf{0}.\end{aligned} \tag{19}$$

Substituting the obtained $\boldsymbol{r}^i$ and $\boldsymbol{p}^i$ into (18a) and only consider the term dependent on $\boldsymbol{\theta}_T$, the sub-problem over $\boldsymbol{\theta}_T$ can be formulated as:

$$\min_{\boldsymbol{\theta}_T,\ \text{s.t.}C2}||\boldsymbol{\theta}_T-(\boldsymbol{r}^i-\rho^{-1}\boldsymbol{p}^i)||^2. \tag{20}$$

Considering the unit-modulus constraint $C3$ and according to [15], the optimal value of $\boldsymbol{\theta}_T$ to minimize sub-problem (20) can be expressed as follows:

$$[\boldsymbol{\theta}_T^{i+1}]_m=\begin{cases}\frac{[\boldsymbol{r}^i-\rho^{-1}\boldsymbol{p}^i]_m}{|[\boldsymbol{r}^i-\rho^{-1}\boldsymbol{p}^i]_m|}, & \text{if } [\boldsymbol{r}^i-\rho^{-1}\boldsymbol{p}^i]_m\neq0\\[\boldsymbol{\theta}_T^i]_m, & \text{otherwise,}\end{cases} \tag{21}$$

where $[\boldsymbol{\theta}_T]_m$ denotes the mth element of $\boldsymbol{\theta}_T$.

Then, substituting $\boldsymbol{\theta}_T^{i+1}$ and $\boldsymbol{p}^i$ into (18b) and considering the first-order derivation condition, we can obtain the following solution:

$$2\boldsymbol{\Phi}\boldsymbol{r}^{i+1}-2\boldsymbol{\Psi}-\boldsymbol{p}^i-\rho(\boldsymbol{\theta}_T^{i+1}-\boldsymbol{r}^{i+1})=0, \tag{22}$$

which can be rearranged as:

$$\boldsymbol{r}^{i+1}=(\rho\mathbf{I}+2\boldsymbol{\Phi})^{-1}(2\boldsymbol{\Psi}+\rho\boldsymbol{\theta}_T^i+\boldsymbol{p}^i). \tag{23}$$

where $\mathbf{I}\in\mathbb{C}^{M\times M}$ denotes the identity matrix.

Lastly, we can obtain the value of $\boldsymbol{p}$ from (18c). Thus, by iteratively optimizing the values of $\boldsymbol{r}$, $\boldsymbol{\theta}_T$, and $\boldsymbol{p}$, we can

optimize the variables of problem (16a). The convergence of the ADMM algorithm can be guaranteed as shown in [16] if the value of the penalty parameter ρ satisfies:

$$\frac{\rho \mathbf{I}}{2} - \mathbf{\Phi} \geq 0. \tag{24}$$

The proposed AO algorithm in our work can converge to a stationary point because the optimizations of $\mathbf{\Theta}_T$ and $\boldsymbol{w}$ will at least not increase the value of the cost function at each iteration. Thus, the cost function will not increase during the alternating optimization process. Thus, the proposed scheme can converge to a stationary point.

C. Complexity analysis

According to [15], the complexity of ADMM algorithm is $\mathcal{O}(T_{\text{ADMM}}M^2 + M^3)$, where T_{ADMM} defines the iteration numbers for the ADMM algorithm and M defines the number of elements of ITS. As such, the complexity of the proposed algorithm is $T_{\text{AO}}\mathcal{O}(T_{\text{ADMM}}M^2 + M^3)$, where T_{AO} is the number of iterations of the AO algorithm.

IV. Simulation Results

This section presents the simulation results to demonstrate the effectiveness of the proposed algorithm. In the simulations, the BS is equipped with four antennas and the ITS consists of 64 elements with $M_x = M_y = 8$. There are two mainlobes pointed to two users and the desired directions are $(\delta_{m_1}, \phi_{m_1}) = (-40°, 0°)$ and $(\delta_{m_2}, \phi_{m_2}) = (50°, 0°)$, respectively. Also, the width of the slack region for the mainlobe is set to $10°$ as in [6]. Then, the left regions outside the two slack regions are the sidelobes. The discrete angle values in the sidelobe regions are sampled at $1°$. In addition, the trade-off parameter is set to $\beta = 0.8$, and the desired beam response in the mainlobe region is set to $D(\delta, \phi) = 1$.

We compare the system performance of the proposed scheme with the following benchmark schemes:

1) *Scheme with random $\boldsymbol{w}$ and $\mathbf{\Theta}_T$*: In this scheme, the cost function for the beam response is not optimized, and the beamforming vector at the BS and the phase shifts of the ITS are generated with random values.
2) *Scheme with discrete phase shifts of the* ITS: The phase shifts of the ITS are generated and optimized as some discrete values as studied in [17]. The set of the discrete values is given as $\mathcal{S}_\Theta = \exp(j\alpha_m)$, $\alpha_m \in \{0, \frac{2\pi}{L}, ..., \frac{2\pi(L-1)}{L}\}$, $\forall m \in [1, M]$, where $L = 2^{b_0}$, b_0 is the number of bits used for phase resolutions . Specially, we set $b_0 = 1$ here.

A. The convergence of the proposed algorithm

In this subsection, we examine the convergence property of J_{LS} in the proposed and benchmark schemes. From Fig. 2, we can see that the value of the cost function decreases as the number of iterations increases and becomes stabilized when the number of iterations reaches approximately 8 in the proposed scheme and the scheme with discrete phase shifts. In addition, the minimum values of J_{LS} in these two schemes are all close to 0, which are significantly lower than the scheme with random $\mathbf{\Theta}_T$ and $\boldsymbol{w}$.

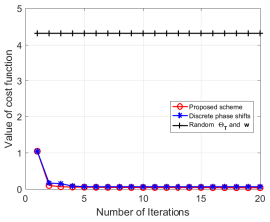

Fig. 2: The convergence behavior of J_{LS} in the proposed and benchmark schemes.

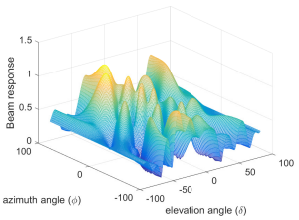

Fig. 3: The beam response of the scheme with random $\boldsymbol{w}$ and $\mathbf{\Theta}_T$.

B. The beam response of the ITS-assisted transmitter

In this subsection, we compare the beam response of the transmit beam in the proposed scheme with the benchmark schemes. We first consider the beam response of the scheme with random $\boldsymbol{w}$ and $\mathbf{\Theta}_T$ as shown in Fig. 3. It can be seen that there are many sidelobes in the beam response, and the mainlobes can not be distinguished clearly. Next, we consider the beam response of the scheme with discrete phase shifts in Fig. 4. In this scheme, the sidelobes are suppressed and the responses of the two mainlobes are close to 1. In addition, the directions of the two mainlobes point to $(-41°, 0°)$ and $(45°, 0°)$, which are close to the desired directions. However, the sidelobes close to the mainlobes are still high. To compare with the benchmark schemes, the beam response of the proposed scheme is shown in Fig. 5. It can seen that the sidelobes are further suppressed effectively and the beam response of two mainlobes are close to 1. Also, the directions of two mainlobes point to $(-40°, 0°)$ and $(49°, 0°)$, which are closer to the desired directions than the scheme with discrete phase shifts. Thus, the optimization of phase shifts is essential to suppress the sidelobes.

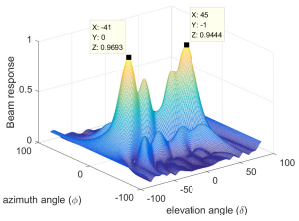

Fig. 4: The beam response of the scheme with discrete phase shifts.

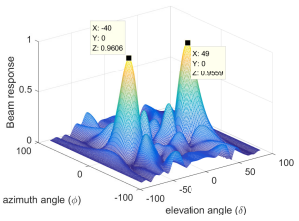

Fig. 5: The beam response of the proposed scheme.

C. The beam response of the fully-digital transmitter

In this subsection, we study the beam response of the scheme with the fully-digital transmitter as shown in Fig. 6 and Fig. 7. When the number of the active antennas in the fully-digital transmitter is 4, it can be seen that the beam response is inferior compared to the proposed scheme. The sidelobes can not be suppressed, and the mainlobes can not point to the desired directions. When the number of active antennas is 64, the same as the passive elements in the proposed scheme, the sidelobes can be suppressed more effectively, and the mainlobes can point to the desired directions. However,

the fully-digital transmitter will incur high cost and power consumption because the massive RF chains are needed [8].

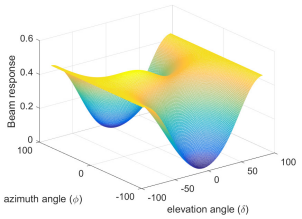

Fig. 6: The beam response of the scheme without ITS ($N = 4$).

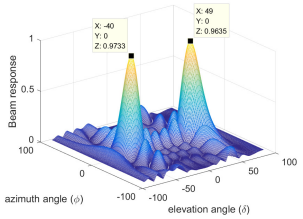

Fig. 7: The beam response of the scheme without ITS ($N = 64$).

D. The spectral efficiency of the transmit beam

Next, we investigate the spectral efficiency of the transmit beam, which can be calculated as:

$$R_{tb}(\delta, \phi) = \log\left(1 + \frac{\mathcal{P}(\delta, \phi) X_t}{\sigma^2}\right), \tag{23}$$

where $X_t = 30$ dBm is the transmit power at the BS and $\sigma^2 = -90$ dBm is the noise power at the ITS-assisted transmitter. In particular, the desired azimuth angles of two users are set to $\phi = 0$. Thus, we consider the simulation results with different elevation angles δ as shown in Fig. 6. It can be seen that the spectral efficiency of the proposed scheme can be maximized at the desired directions. However, the high values of the sidelobes in the scheme with discrete phase shifts will interfere with the mainlobes, which may affect the information transmission. Especially, the performance of the scheme with the random values is worse.

V. Conclusion

This letter considered the minimization of the cost function J_{LS} based on LS to suppress the high sidelobes for a wireless network with the proposed ITS-assisted transmitter structure. To solve the minimization problem, we applied the AO and ADMM algorithms to optimize the digital beamforming vector at the BS and the phase shifts of the ITS in an alternative manner. Then, we obtained the optimized beam response where the sidelobes are suppressed effectively and the mainlobes pointed to the desired directions towards the intended users accurately as shown by the simulation results. Compared with other benchmark schemes, we demonstrated the improvement of the proposed scheme in terms of beam response and the spectral efficiency of the transmit beam. For our future work, we will analyze the performance benefits of sidelobe suppression in the multi-cell environments.

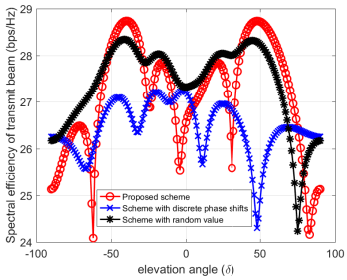

Fig. 8: The spectral efficiency of the transmit beam with different elevation angles.

References

[1] O. El Ayach, S. Rajagopal, S. Abu-Surra, Z. Pi, and R. W. Heath, "Spatially sparse precoding in millimeter wave MIMO systems," *IEEE Trans. Wireless Commun.*, vol. 13, no. 3, pp. 1499–1513, 2014.

[2] J. Li, X. Li, L. Xiao, and S. Zhou, "Joint Multi-Beam and Channel Tracking for mmWave Hybrid Beamforming Multi-User Systems," *IEEE Wireless Commun. Lett.*, vol. 10, no. 7, pp. 1513–1517, 2021.

[3] H. Yan, S. Ramesh, T. Gallagher, C. Ling, and D. Cabric, "Performance, power, and area design trade-offs in millimeter-wave transmitter beamforming architectures," *IEEE Circuits Syst. Mag.*, vol. 19, no. 2, pp. 33–58, 2019.

[4] B. Ning, Z. Chen, X. Wang, and W. Mei, "Codebook-based hybrid beamforming design for MISOME wiretap channel," *IEEE Wireless Commun. Lett.*, vol. 8, no. 1, pp. 57–60, 2018.

[5] M. Shimizu, "Millimeter-wave beam multiplexing method using subarray type hybrid beamforming of interleaved configuration with inter-subarray coding," *Int. J. Wireless Inf. Networks*, vol. 24, no. 3, pp. 217–224, 2017.

[6] J. Zhang, W. Liu, C. Gu, S. S. Gao, and Q. Luo, "Multi-beam multiplexing design for arbitrary directions based on the interleaved subarray architecture," *IEEE Trans. Veh. Technol.*, vol. 69, no. 10, pp. 11220–11232, 2020.

[7] J. Zhang and W. Liu, "Antenna Selection for Multi-Beam Multiplexing Design Based on the Hybrid Beamforming Architecture," in *2021 IEEE Statistical Signal Processing Workshop (SSP)*, pp. 261–265, IEEE, 2021.

[8] V. Jamali, A. M. Tulino, G. Fischer, R. R. Müller, and R. Schober, "Intelligent surface-aided transmitter architectures for millimeter-wave ultra massive MIMO systems," *IEEE Open J. Commun. Soc.*, vol. 2, pp. 144–167, 2020.

[9] N. Shlezinger, G. C. Alexandropoulos, M. F. Imani, Y. C. Eldar, and D. R. Smith, "Dynamic metasurface antennas for 6G extreme massive MIMO communications," *IEEE Wireless Commun.*, vol. 28, no. 2, pp. 106–113, 2021.

[10] W. Tang, J. Y. Dai, M. Z. Chen, K.-K. Wong, X. Li, X. Zhao, S. Jin, Q. Cheng, and T. J. Cui, "MIMO transmission through reconfigurable intelligent surface: System design, analysis, and implementation," *IEEE J. Sel. Areas Commun.*, vol. 38, no. 11, pp. 2683–2699, 2020.

[11] Z. Yang, W. Xu, C. Huang, J. Shi, and M. Shikh-Bahaei, "Beamforming design for multiuser transmission through reconfigurable intelligent surface," *IEEE Trans. Commun.*, vol. 69, no. 1, pp. 589–601, 2020.

[12] S. Doclo and M. Moonen, "Design of broadband beamformers robust against gain and phase errors in the microphone array characteristics," *IEEE Trans. Signal Process.*, vol. 51, no. 10, pp. 2511–2526, 2003.

[13] Q. Wu, S. Zhang, B. Zheng, C. You, and R. Zhang, "Intelligent reflecting surface-aided wireless communications: A tutorial," *IEEE Trans. Commun.*, vol. 69, no. 5, pp. 3313–3351, 2021.

[14] Y. Wang, W. Yin, and J. Zeng, "Global convergence of admm in nonconvex nonsmooth optimization," *J. Sci. Comput.*, vol. 78, no. 1, pp. 29–63, 2019.

[15] H. Niu, Z. Chu, F. Zhou, Z. Zhu, M. Zhang, and K.-K. Wong, "Weighted sum secrecy rate maximization using intelligent reflecting surface," *IEEE Trans. Commun.*, vol. 69, no. 9, pp. 6170–6184, 2021.

[16] H. Guo, Y.-C. Liang, J. Chen, and E. G. Larsson, "Weighted sum-rate optimization for intelligent reflecting surface enhanced wireless networks," *arXiv preprint arXiv:1905.07920*, 2019.

[17] P. Xu, G. Chen, Z. Yang, and M. Di Renzo, "Reconfigurable intelligent surfaces-assisted communications with discrete phase shifts: How many quantization levels are required to achieve full diversity?," *IEEE Wireless Commun. Lett.*, vol. 10, no. 2, pp. 358–362, 2020.